Vietnam Journal of Earth Sciences, 44(1), 1-17, https://doi.org/10.15625/2615-9783/16315

Vietnam Academy of Science and Technology
**Vietnam Journal of Earth Sciences**
http://www.vjs.ac.vn/index.php/jse

# Monitoring spatial-temporal dynamics of small lakes based on SAR Sentinel-1 observations: a case study over Nui Coc Lake (Vietnam)

Pham Duc Binh*, Tong Si Son

*University of Science and Technology of Hanoi, VAST, Hanoi, Vietnam*

Received 10 May 2021; Received in revised form 09 July 2021; Accepted 15 July 2021

ABSTRACT

For the first time, this study estimates the variation of surface water extent of Nui Coc Lake located in Thai Nguyen province in North Vietnam at high spatial (20m) and temporal resolution (bi-weekly). The classification methodology was developed based on the Otsu threshold algorithm applied to histogram of the backscatter coefficient of the SAR Sentinel-1 signal. Totally, more than 150 SAR Sentinel-1 images have been processed for the 2016-2020 period. Except for extreme drought and flood conditions, the average minimum and maximum of the lake's surface water extent are 17 $km^2$ (in May) and 24 $km^2$ (in September/October), respectively, and Nui Coc Lake's surface water was stable during the last five years. Classification results are in good agreement with the corresponding surface water extent maps derived from free-cloud Sentinel-2 images, with the occurrence map derived from the Landsat-derived Global Surface Water (GSW) product, and with in situ precipitation data. Compared to Sentinel-2, the lake's surface water extent detected from Sentinel-1 is 4-4.5% less. The water occurrence is similar between our results and that derived from the GSW product, but Sentinel-1 observations provide more details as its spatial resolution is higher than Landsat. This study clearly shows the great potential of SAR Sentinel-1 data for monitoring small lake's water surface at low costs, especially over tropical regions.

*Keywords:* Lake surface water monitoring, Nui Coc Lake (Vietnam), SAR, Sentinel-1.

## 1. Introduction

Lakes and reservoirs are often among the most critical water resources on Earth, providing a large part of our freshwater (Crétaux et al., 2016; Huth et al., 2020). They are essential for ecosystems and play irreplaceable roles in human survival and social development. Monitoring spatial and temporal dynamics of water resources, including lakes and reservoirs, is critically important for water management, especially in developing countries and under the current climate change pressure (Pham-Duc, Prigent, & Aires, 2017). Reliable information about the spatial and temporal distribution of lakes and reservoirs can be of great interest in many scientific disciplines, such as the assessment of present and future water resources, climate models, flood mapping, environment

*Corresponding author, Email: pham-duc.binh@usth.edu.vn

monitoring, wetland inventory, and water management (Williamson, Saros, Vincent, & Smol, 2009). Despite their importance, lakes and reservoirs have been considered as a minor part of the biosphere. Therefore, until recently, their contributions were normally ignored in global estimations of ecosystem processes (Downing et al., 2006).

There are a few comprehensive lake databases that provide statistical information related to the location, size, extent, and dynamics of wetlands, lakes, and reservoirs on a global scale (Downing et al., 2006; Lehner & Döll, 2004; McDonald, Rover, Stets, & Striegl, 2012). Thanks to the fast development in remote sensing, satellite observations have been used to estimate global wetlands and lakes with higher accuracy and spatial resolution (Pekel, Cottam, Gorelick, & Belward, 2016; Verpoorter, Kutser, Seekell, & Tranvik, 2014). However, these databases were developed using optical satellite observations, which are greatly affected by cloud contamination. This constraint reduces applications of these datasets in some regions (e.g., in the Tropics).

Synthetic Aperture Radar (SAR) satellite data are a highly suitable source for mapping and monitoring variation of lake surface water as SAR sensors allow observations regardless of the cloud cover, day and night, with spatial and temporal resolutions comparable to optical remote sensing (Brisco et al., 2008). There are several earth observation satellites equipped with SAR sensors that are suited for surface water detection and monitoring, including the European ENVISAT ASAR, the Canadian Radarsat-1/2, the Japanese ALOS Palsar, the Italian COSMO-SkyMed, the German TerraSAR-X/TanDEM-X, and most recently, the European Space Agency (ESA) Sentinel-1A/B (Moreira et al., 2013). SAR observations have been employed extensively in many studies for monitoring floods (Martinis et al., 2015; Pierdicca, Pulvirenti, Chini, Guerriero, & Candela, 2013; Voormansik, Praks, Antropov, Jagomagi, & Zalite, 2014), for surface water monitoring (Bartsch, Pathe, Wagner, & Scipal, 2008; Brisco, Short, van der Sanden, Landry, & Raymond, 2009; Reschke, Bartsch, Schlaffer, & Schepaschenko, 2012), and for lake monitoring (Huth et al., 2020). These studies mainly focused on local scales because of the lack of global SAR observations and that it is not easy to freely access all available SAR observations. The first global water map derived from multi-year (2002-2012) ENVISAT ASAR observations at 150 m spatial resolutions has been published recently in 2015 (Santoro et al., 2015). Although small lakes are numerically dominant (Downing et al., 2006), their water occurrence is insignificantly investigated using SAR data. Additionally, small lakes in tropical weather are temporally covered by floating vegetation, making serious bias for determining its surface water extent using a single satellite image.

This study aims to investigate the use of SAR Sentinel-1 observations to frequently monitor dynamics of small lakes in tropical areas, where in situ measurements of small lakes' surface water are normally not available due to the lack of financial support, at high spatial (20 m) and temporal resolutions (bi-weekly). Nui Coc Lake, one of the most important reservoirs located in Thai Nguyen province in North Vietnam, has been selected as the test site. Section 2 describes the study area, Sentinel-1 data, and other ancillary data used in this study. Pre- and post-processing steps and the classification methodology are presented in Section 3. Results and comparisons with other surface water products are shown and discussed in Section 4. Section 5 concludes this study and introduces possible further work.

## 2. Study Area and Materials

### *2.1. Study Area - Nui Coc Lake in the North Vietnam*

Nui Coc Lake is an artificial lake, located in the southwest of Thai Nguyen Province in

North Vietnam, between latitudes 21.52°N-21.62°N and longitudes 105.64°E-105.74°E (Fig. 1). The lake was built during the 1973-1982 period, by the construction of a dam to block the Cong River in the middle of the mountain. The lake includes the main dam of 480 m long, and seven auxiliary dams. Nui Coc Lake has a depth of 50 m, with an average surface water area of 24-25 $km^2$ and a capacity of 175 million $m^3$ (Duong, 2012). As the biggest irrigation works in Thai Nguyen, Nui Coc Lake and its ancillary works formed an irrigation system that is responsible for supplying irrigation water for 120 $km^2$ of paddy rice in Thai Nguyen City, Thai Nguyen industrial park, and four other districts, with the average discharge of 30 $m^3/s$. In addition, Nui Coc Lake is the main water supply for Thai Nguyen city, with a total volume from 40-70 million $m^3$/year. Nui Coc Lake also works as a detention reservoir to control droughts and floods for Thai Nguyen and the surrounding areas. During drought periods, the lake replenishes water for the Song Cau irrigation system, while during flood periods, the lake helps to cut floods in the lower Cong River basin. The region is characterized by a tropical monsoon climate with a cold-dry winter from November to April, and a hot, humid, and rainy summer from May to October. The average annual temperature varies between 21.5°C and 23°C, while the average annual rainfall is in the range of 2,000 to 2,500 mm, highest in August and lowest in January (Tran, 2020).

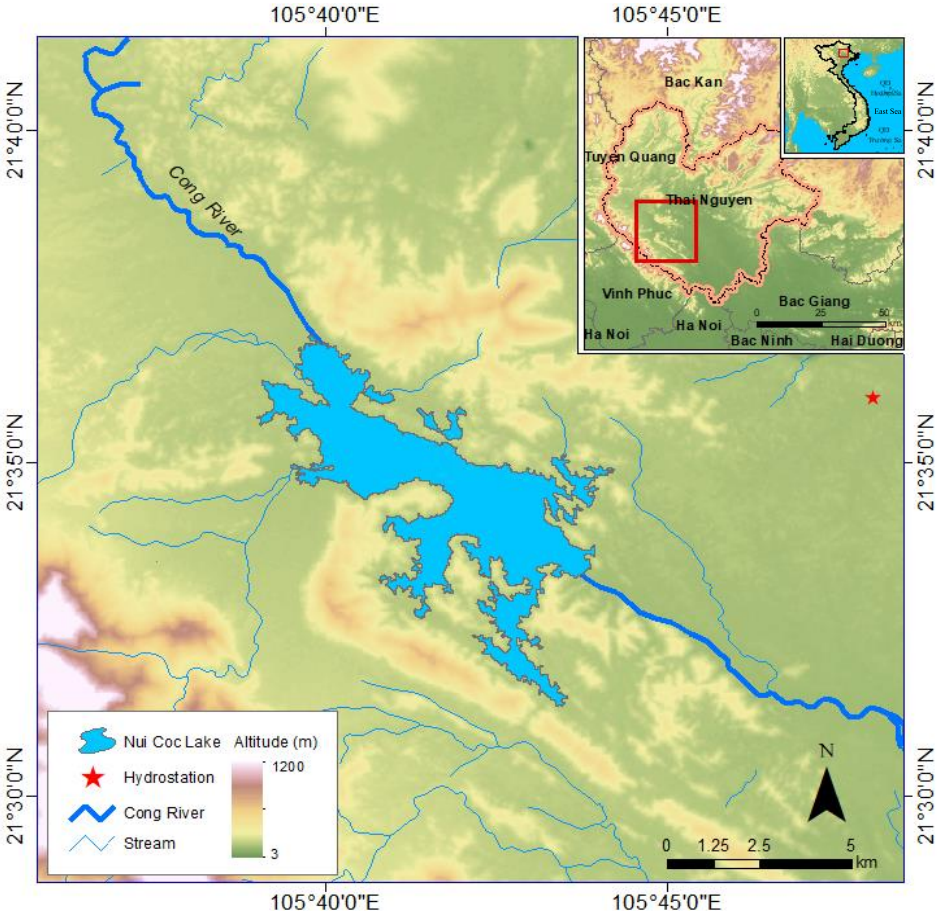


*Figure 1*. Location of Nui Coc Lake in Thai Nguyen province, located in the North Vietnam

### *2.2. Sentinel-1 SAR Data*

The ESA Sentinel-1 project includes two identical SAR satellites (1A and 1B) working at C-band (5.405 GHz) with the main objective of observing and monitoring Earth's land and ocean surfaces day and night, under all weather conditions. Sentinel-1A satellite was launched on April 3, 2014, and Sentinel-1B was launched on April 22, 2016. The mission provides a re-visiting time of 6 days (12 days with only one satellite). Due to the lack of Sentinel-1B data in the study area, we only used Level-1 Sentinel-1A Ground Range Detected (GRD) from the Interferometric WideSwath (IW) mode at 20 m spatial resolution. The standard GRD product contains amplitude information in dual-polarized default operation mode: vertically transmitted and horizontally received (VH), and vertically transmitted and vertically received (VV). As the VH polarization is more sensitive to the presence of water (Ottinger et al., 2017; Pham-Duc et al., 2017), VV polarization images were not used in this study. The period 2016-2020 was selected as VH polarization was not available before 2016 in the study area. Sentinel-1 imagery was downloaded free-of-charge from the Sentinel Data Hub (https://scihub.copernicus.eu/dhus/#/home).

### *2.3. Ancillary Datasets*

#### *2.3.1. Surface Water Maps Derived from Sentinel-2 Data*

Sentinel-2 is an ESA's wide-swath, high-resolution, multi-spectral imaging mission, designed for land monitoring studies, including monitoring soil, water, and vegetation at a maximum 10 m spatial resolution. Sentinel-2A&B was launched on June 23, 2015, and March 7, 2017, respectively. In this study, we used the Modified Normalized Difference Water Index (MNDWI) (Xu, 2006) for detecting surface water extent of Nui Coc Lake as this index performs better there for water body detection, compared to the Normalized Difference Water Index (NDWI) (Tran, 2020). Sixteen free-cloud Sentinel-2 Level-1C (Top-of-Atmosphere) and Level-2A (Bottom-of-Atmosphere) images are selected to build the surface water extent maps to compare with the corresponding maps derived from SAR Sentinel-1 images. Sentinel-2 imagery was also downloaded freely from the Sentinel Data Hub. The list of 16 Sentinel-1/Sentinel-2 image pairs used in this study and the differences (in days) between their acquisitions is shown in Table 1.

*Table 1.* List of 16 pairs of SAR Sentinel-1 and free-cloud Sentinel-2 observations used in this study

| Date of Acquisition | | | |
|---|---|---|---|
| Image No | Sentinel-1 | Sentinel-2 | Day Gap |
| 1 | November 03 2017 | October 31 2017 | 3 |
| 2 | December 21 2017 | December 20 2017 | 1 |
| 3 | January 14 2018 | January 19 2018 | 5 |
| 4 | March 15 2018 | March 10 2018 | 5 |
| 5 | April 08 2018 | April 09 2018 | 1 |
| 6 | September 23 2018 | September 21 2018 | 2 |
| 7 | October 05 2018 | October 06 2018 | 1 |
| 8 | October 29 2018 | October 31 2018 | 2 |
| 9 | May 21 2019 | May 19 2019 | 2 |
| 10 | September 06 2019 | September 06 2019 | 0 |
| 11 | September 30 2019 | October 01 2019 | 1 |
| 12 | November 05 2019 | November 05 2019 | 0 |
| 13 | November 29 2019 | December 05 2019 | 6 |
| 14 | December 11 2019 | December 10 2019 | 1 |
| 15 | March 04 2020 | March 09 2020 | 5 |
| 16 | November 11 2020 | November 09 2020 | 2 |

*2.3.2. Global Surface Water*

The Global Surface Water (GSW) dataset (Pekel et al., 2016), developed by the European Commission's Joint Research Centre, maps the location and temporal distribution of water surfaces globally and provides variations of those water surfaces. The dataset was produced using 36 years of Landsat imagery at 30 m spatial resolution (1984-2019). The GSW dataset provides six different types of maps, including occurrence, change, seasonality, recurrence, transitions, and maximum extent of surface water. In this study, the occurrence and maximum extent maps of 2019 were used to compare to results derived from SAR Sentinel-1 imagery. The GSW dataset is freely available at: https://global-surface-water.appspot.com/#.

*2.3.3. Daily In Situ Precipitation Data*

In situ daily precipitation data from the Thai Nguyen hydro-meteorological station (21.6°N; 105.8°E) are collected to compare with our surface water extent maps derived from SAR Sentinel-1 imagery. Data collection can be requested from the Vietnam Meteorological and Hydrological Administration, available at: http://kttvqg.gov.vn/.

## 3. Methodology

### *3.1. Lake Surface Water Extraction from Sentinel-1 Observations*

*3.1.1. Sentinel-1 GRD Image Processing Chain*

Sentinel-1 GRD processing chain includes two parts: pre-and post-processing. In the pre-processing part, the Graph Builder tool within the ESA's open-source software SNAP (SeNitnel's Application Platform) was utilized, following the processing steps presented in Fig. 2 (ESA, 2016; Filipponi, 2019). Note that only Sentinel-1 VH polarization images were processed (Ottinger et al., 2017; Pham-Duc et al., 2017). First, each image is spatially cropped to the area that fully covers Nui Coc Lake (21.48°-21.66°N; 105.62°-105.80°E) to reduce the processing time. Second, Apply Orbit File is applied to update and correct the orbit state vectors for each Sentinel-1 scene, providing an accurate satellite position and velocity information. Third, each image is calibrated to convert digital values at each pixel to radiometrically calibrated backscatter. Fourth, Speckle Filter is applied to improve image quality by reducing the speckle noise. Several filters are available (i.e., Lee, Lee Sigma, Refined Lee, and Median), but results derived from these filters showed little differences in surface water detection (Pham-Duc et al., 2017). Finally, the Refined Lee filter was chosen as this filter maintains the standing water boundary (C. Liu, 2016). Next, Terrain Correction is applied to compensate for the distortions caused by the side-looking geometry of the satellite. As a result, the geometric representation of the image will be as close as possible to the real world. The last preprocessing step is to convert the unitless backscatter coefficient of the image to dB for better interpretation, using a logarithmic transformation provided in the "Linear to from dB" function. After the pre-processing steps, all Sentinel-1 output products are post-processed by applying the SNAP's Coregistration tool. The main objective of the post-processing step is to spatially collocate all Sentinel-1 images into one geographic projection with the same geo-positioning information and similar image dimensions. Fig. 3 (left) shows an example of the final Sentinel-1 product after being processed, with Nui Coc Lake appears very dark. At this step, Sentinel-1 images are ready as input for the classification.

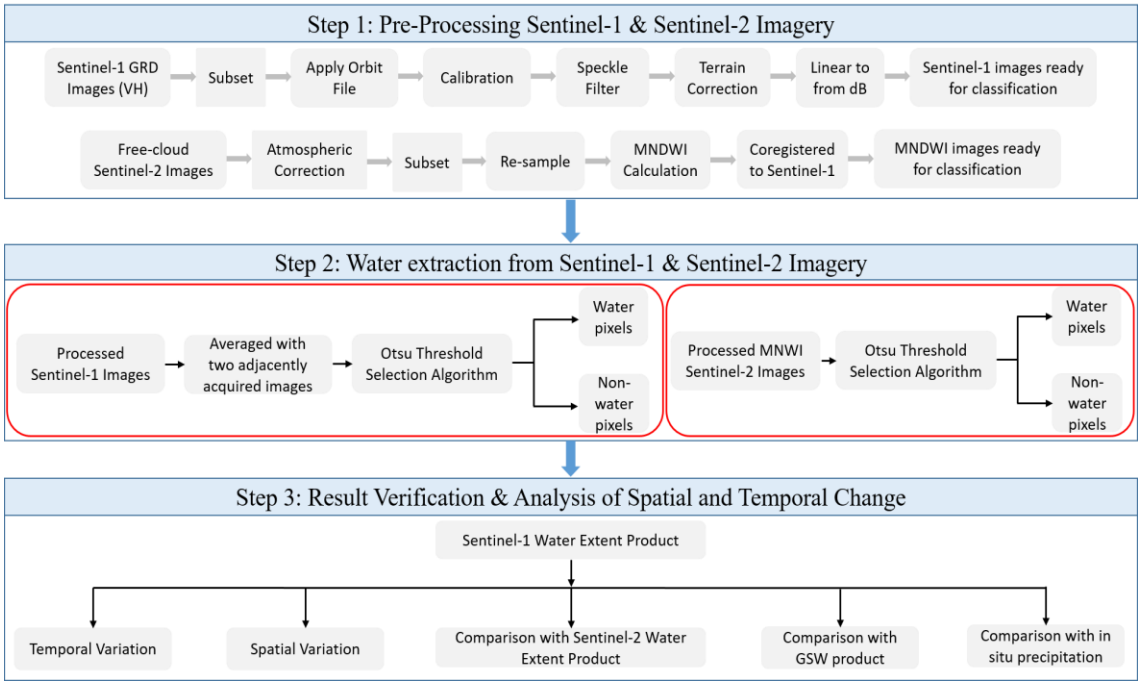


*Figure 2.* The technical framework diagram of this study

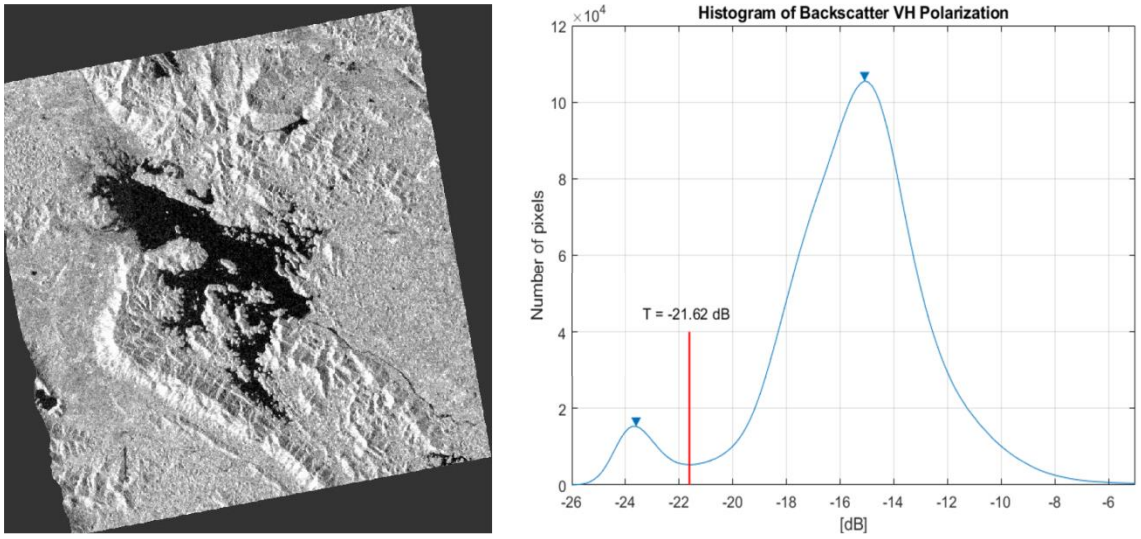


*Figure 3.* Example of processed Sentinel-1 image at VH polarization (left), and its histogram (right). The red line indicates the optimal threshold (T = -21.62 dB), detected using the Otsu threshold method. Sentinel-1 observations were acquired on March 22, 2019

### *3.1.2. Surface Water Extraction*

Our classification algorithm is based on the fact that calm water surfaces usually act like mirrors and reflect almost incoming microwave radiation into the specular direction. Therefore, over water surfaces, the return pulses to the satellite sensors are normally feeble, making the backscatter coefficient over water surfaces are very low

(Kuenzer et al., 2013; Pierdicca et al., 2013). Threshold classification was reported to have high accuracy (between 85%-96%) in detecting water and non-water pixels (Martinis et al., 2015). However, its accuracy can be affected by several mechanisms. Strong winds can cause roughness on water surfaces, leading to a stronger return pulse on the satellite sensors, and making higher values of backscatter coefficient over water surfaces (Gstaiger, Huth, Gebhardt, Wehrmann, & Kuenzer, 2012). Double-bounce scattering mechanism over aquatic vegetation (Hess, et al., 1990; Pope et al., 1997), or volume scattering of vegetation canopy over water surfaces (e.g., rice paddy) might also enhance the backscatter coefficient (Y. Liu et al., 2016). To reduce noises and increase the accuracy of the methodology, each Sentinel-1 image was averaged with the two adjacently acquired images before the final classification step. Fig. 3 (right) shows the histogram of the backscatter at VH polarization of the processed Sentinel-1 image on the left. Two peaks can be seen clearly: the lower one corresponds to water pixels, and the higher one corresponds to non-water pixels. The Otsu threshold selection method (Otsu, 1979) is applied to each Sentinel-1 image to identify the optimal threshold value for separating water and non-water pixels. The optimal threshold varies from one image to another, but the mean value is -21.8 dB with a standard deviation of 0.37 dB.

### *3.2. Lake Surface Water Extraction from Sentinel-2 Observations*

Several pre-processing steps are applied to all 16 free-cloud Sentinel-2 images over the study area, as shown in Fig. 2. First, Sentinel-2 Level-1C Top-of-Atmosphere (TOA) products are atmospherically corrected to Level-2A Bottom-of-Atmosphere (BOA) using the Sen2Cor tool (Louis et al., 2016). Then, each Sentinel-2 image is spatially cropped to the same area as Sentinel-1 before being re-sampled to 10 m spatial resolution using the SNAP software. The MNDWI at the pixel level is calculated using Equation 1 (Xu, 2006).

$$MNDWI = \frac{GREEN - SWIR}{GREEN + SWIR} \quad (1)$$

where GREEN and SWIR are the BOA reflectance at 10 m spatial resolution of the green band (band 3 at 560 nm) and the short wavelength infrared band (band 11 at 1610 nm). Next, the MNDWI images are coregistered to the corresponding Sentinel-1 images so that all Sentinel-1/Sentinel-2 image pairs have the same geographic projection and image dimensions for comparison. Finally, the Otsu threshold selection method is applied for all MNDWI images to extract the water extent map.

## 4. Results

### *4.1. Surface Water Variation of Nui Coc Lake Derived from Sentinel-1 Imagery*

The variation of surface water of Nui Coc Lake during the 2016-2020 period, derived from more than 150 Sentinel-1A observations, is shown in Fig. 4. As the temporal resolution of the satellite is 12 days, there are normally 2-3 images per month. Surface water area of Nui Coc Lake is quite stable over the last five years, except during summer of 2017 when the surface water extent decreased significantly to nearly 10 $km^2$. As monthly time series of area-averaged of merged satellite-gauge precipitation estimate (GPM 3IMERGM v06 product) over Nui Coc Lake, provided by NASA Earth Data's Giovanni (Acker & Leptoukh, 2007) does not observe a decline of accumulated precipitation, we conclude that the extremely low of the lake water extent in 2017 mainly caused by the withdrawn of its water to prepare for the maintenance and repair of the main lake dam in July and August 2017 (Dong, 2017). In

general, the water extent of Nui Coc Lake reaches the maximum level in September/October (after the rainy season) and the minimum level in May (during summer). The minimum and maximum surface water extent of Nui Coc are 17 $km^2$ and 24 $km^2$, respectively. During the two recent years (2019-2020), minimum water extent levels were higher than in previous years. Note that Nui Coc is an artificial lake, and its water is well controlled to support human needs and agriculture activities. Therefore, the lake's water withdrawal speed varies from one year to the others, depending on the dam operation plan. For example, 2020 witnessed a slower lake's water withdrawal compared to other years. Until April 2020, the lake's water extent was still nearly 22 $km^2$, while in other years, the lake's water extent in April was always between 17 and 19 $km^2$.

As 2017 showed the biggest contrast of the lake's water surface between the minimum and the maximum states, its monthly variation is shown in Fig. 5. The monthly variation of Nui Coc Lake's water extent in 2017 followed very well the annual seasonality. The lake's water extent was still being large in January (22 $km^2$). After that, it started to reduce slightly in February and March to 19.2 $km^2$ and 16.2 $km^2$, respectively. Between April and June, the lake's water extent was at the minimum level between 11 and 12 $km^2$ before increasing quickly to reach an extent of 19.5 $km^2$ in August and 22.5 $km^2$ in September. The lake's water extent was at the maximum level in October (23.5 $km^2$). After the peak of the rainy season, its water extent was kept stable for the rest of the year.

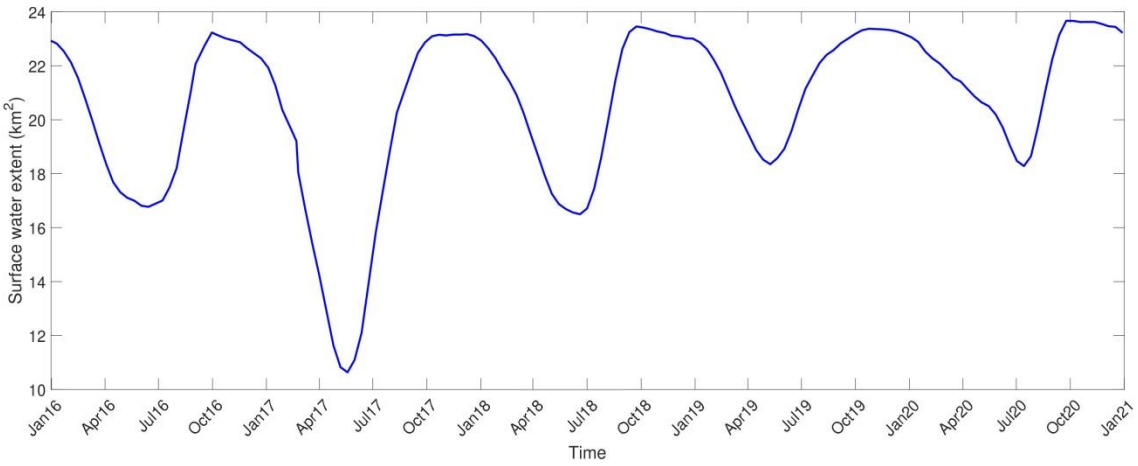


*Figure 4.* Bi-weekly time series of surface water of Nui Coc Lake for the 2016-2020 period

Maps of annual permanent (light blue) and maximum (light and dark blue) of the water extent of Nui Coc Lake for the 2016-2020 period were shown in Fig. 6, while its areas are shown in Table 2. Except for 2017, when the lake's permanent water extent was shallow, other years showed very similar spatial distribution of water surfaces and total inundated areas at both two states. Over the last five years, the maximum surface water extent of Nui Coc Lake varies between 23.5 $km^2$ and 24 $km^2$. The permanent water surfaces in the two recent years (2019-2020) were slightly higher (2 $km^2$) than in 2016 and 2018. Note that a pixel is defined as permanent water if that pixel was classified as water in 90% of Sentinel-1 observations in the year.

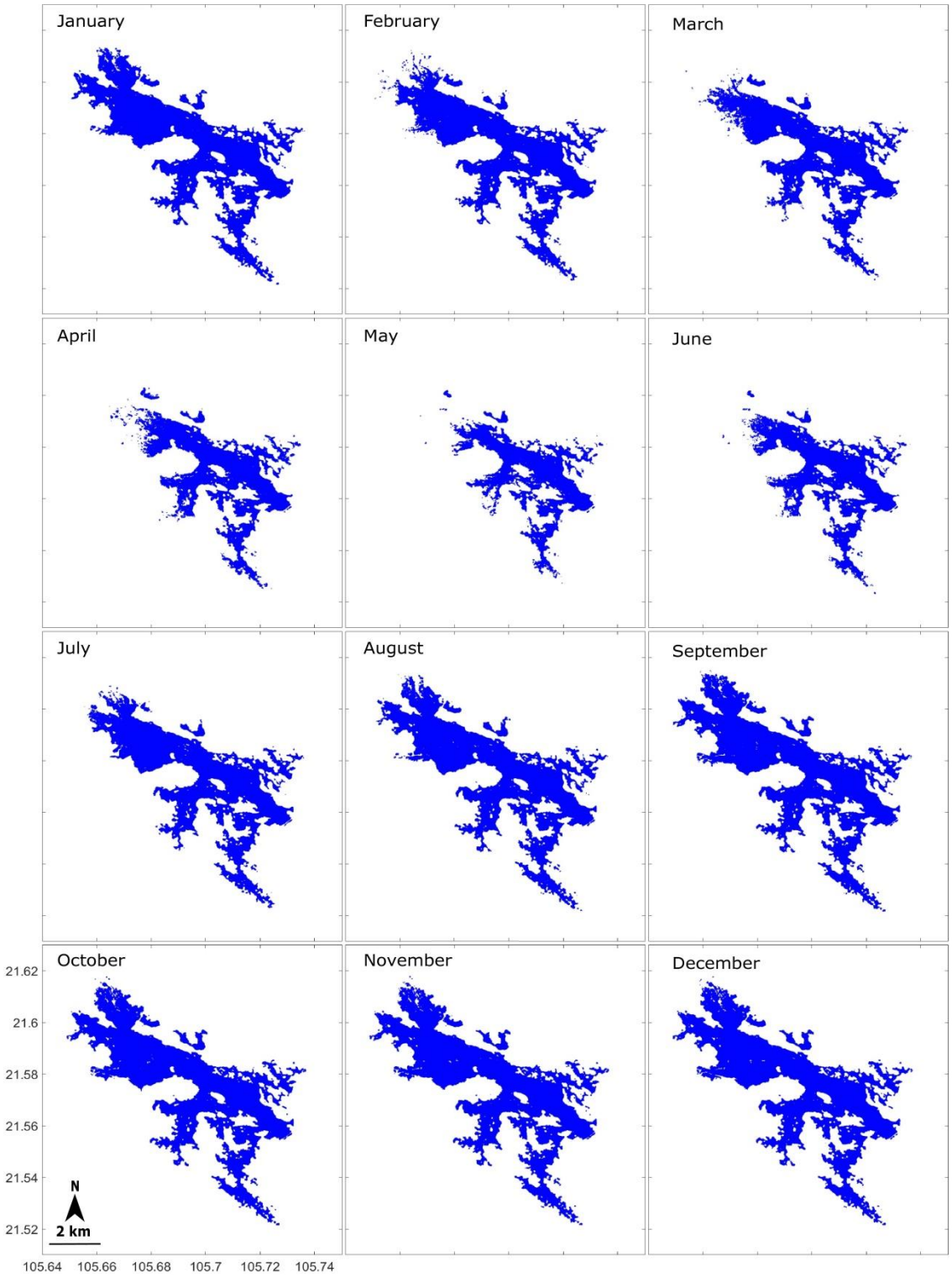


*Figure 5.* Monthly variation of surface water extent of Nui Coc Lake in 2017, derived from Sentinel-1A observations

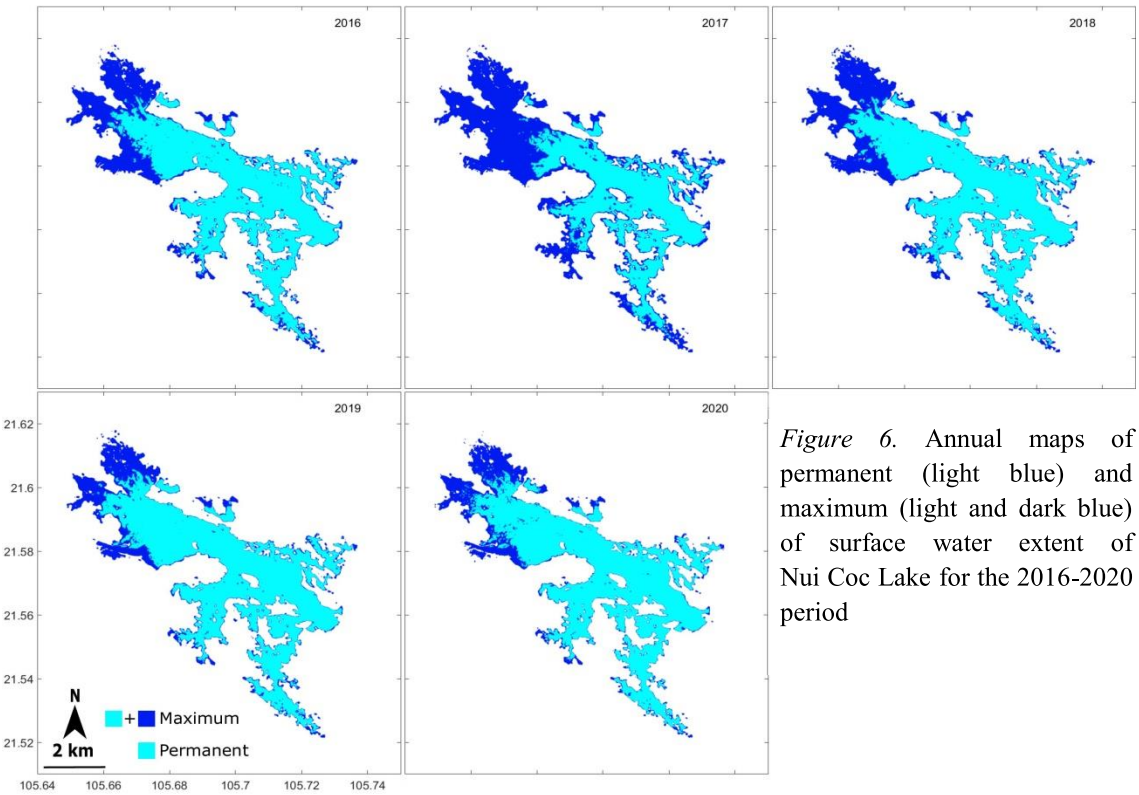


*Figure 6.* Annual maps of permanent (light blue) and maximum (light and dark blue) of surface water extent of Nui Coc Lake for the 2016-2020 period

*Table 2.* Annual permanent and maximum of surface water extent of Nui Coc Lake for the 2016-2020 period

| | Year | | | | |
|---|---|---|---|---|---|
| | 2016 | 2017 | 2018 | 2019 | 2020 |
| Permanent water ($km^2$) | 16.80 | 10.90 | 16.60 | 18.60 | 18.40 |
| Maximum water ($km^2$) | 23.70 | 23.60 | 23.80 | 23.90 | 23.20 |

### *4.2. Comparisons with Sentinel-2 Derived Surface Water Maps*

In this section, Sentinel-1 derived surface water extent maps of Nui Coc Lake are compared with results obtained from the corresponding free-cloud MNDWI images derived from Sentinel-2 observations. Totally, 16 pairs of Sentinel-1/Sentinel-2 images are processed, and some comparisons are presented in Fig. 7 where we show maps of surface water extent of Nui Coc Lake in the dry season (top) and the rainy season (bottom) of 2019, respectively. For the dry season, Sentinel-1 image was acquired on May 21, and Sentinel-2 images were acquired two days before, on May 19. The total water surface detected from the Sentinel-1 image (Fig. 7a) is 18.3 $km^2$, while the number detected from the Sentinel-2 image (Fig. 7a) is 18.1 $km^2$. The confusion matrix is shown in Table 3 (left). The overall agreement of the classification is 99.15%, with a true positive detection of water pixels is 92.7%, and false-negative detection of 7.3%. Compared to the Sentinel-2 map, Sentinel-1 derived surface water extent map classified correctly 99.6% of non-water pixels. For the rainy season, Sentinel-1 image was acquired on September 30, and Sentinel-2 image was acquired one day after, on October 01. The confusion matrix presented in Table 3 (right) shows an overall agreement of 99.3%, with a very high true positive detection of water pixels

(98.7%), and a false-negative detection of 1.3%. Compared to the Sentinel-2 map, the classification method using the Sentinel-1 image detected correctly 99.4% of non-water pixels. The total water surface detected from the Sentinel-1 image is 23.2 km$^2$ (Fig. 7d), compared to 24.8 km$^2$ detected from the Sentinel-2 image (Fig. 7e).

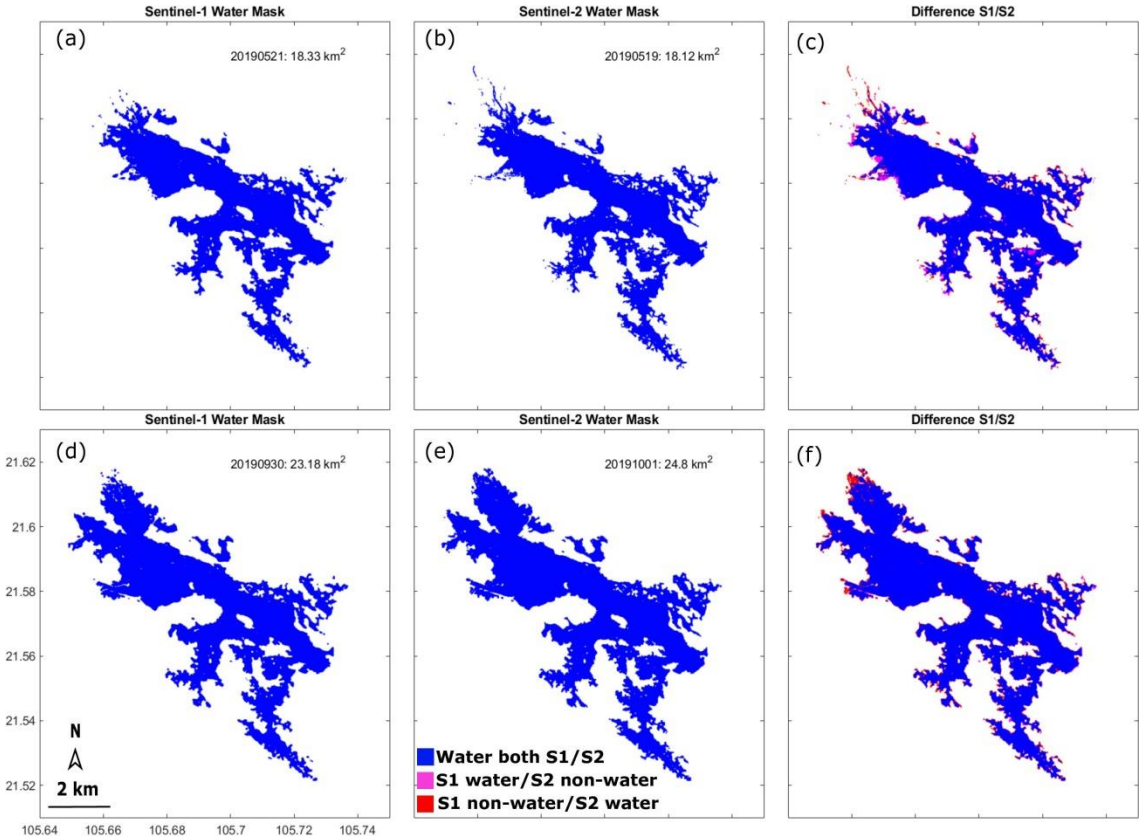


*Figure 7*. (a, d) Sentinel-1 derived surface water maps; (b, e) Sentinel-2 derived surface water maps; and (c, f) their differences of Nui Coc Lake for dry season (top) and rainy season (bottom) of 2019

*Table 3.* Confusion matrices (in numeric and percentage forms) of the surface water extent maps derived from Sentinel-1 and free-cloud Sentinel-2 observations for dry season (top) and rainy season (bottom) of 2019

| **Dry season** | | | **Rainy season** | | |
|---|---|---|---|---|---|
| | **Non-water (0) (Sentinel-2)** | **Water (1) (Sentinel-2)** | | **Non-water (0) (Sentinel-2)** | **Water (1) (Sentinel-2)** |
| **Non-water (0) (Sentinel-1)** | 2,719,186 (99.6%) | 11,227 (0.4%) | **Non-water (0) (Sentinel-1)** | 3,002,911 (99.4%) | 19,422 (0.6%) |
| **Water (1) (Sentinel-1)** | 13,377 (7.3%) | 169,888 (92.7%) | **Water (1) (Sentinel-1)** | 3,192 (1.3%) | 228,625 (98.7%) |

In Fig. 8, a comparison of the lake's water surfaces derived from 16 Sentinel-1/Sentinel-2 image pairs is shown, with the linear registration (red line). There was a good agreement between surface water extent detected from two types of satellite sensors (R = 97%). However, Sentinel-2 images detected more water surfaces than Sentinel-1 images in most cases, with the mean difference of only 1 km$^2$ between the two

surface water maps.

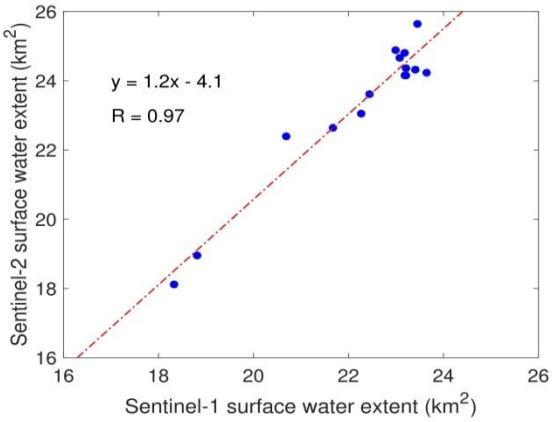


*Figure 8.* Comparison of surface water extent of Nui Coc Lake, derived from 16 pairs of Sentinel-1 and free-cloud Sentinel-2 observations

### *4.3. Comparisons with Landsat Derived Globe Surface Water Product*

Comparisons of permanent (light blue) and maximum (light and dark blue) surface water extent of Nui Coc Lake in 2019, derived from our methodology and the GSW product, are shown in Fig. 9. The shape of Nui Coc Lake is similar in both datasets. Still, higher spatial resolution images from Sentinel-1 observations provide more details than lower spatial resolution images from Landsat. The permanent surface water extent of Nui Coc Lake in 2019, derived from the GSW product, was 16.9 km$^2$, compared to 18.6 km$^2$ detected from our methodology (Table 2). At the maximum state, the water surface detected from the GSW product was higher than from our results (25.4 km$^2$ compared to 23.9 km$^2$). Inundation frequency maps of Nui Coc Lake, derived from 5 years (2016-2020) of Sentinel-1 observations and 36 years (1984-2019) of Landsat observations, are shown in Fig. 10, which clearly identify the most dynamic parts of the lake in the northern part and along the land/water border.

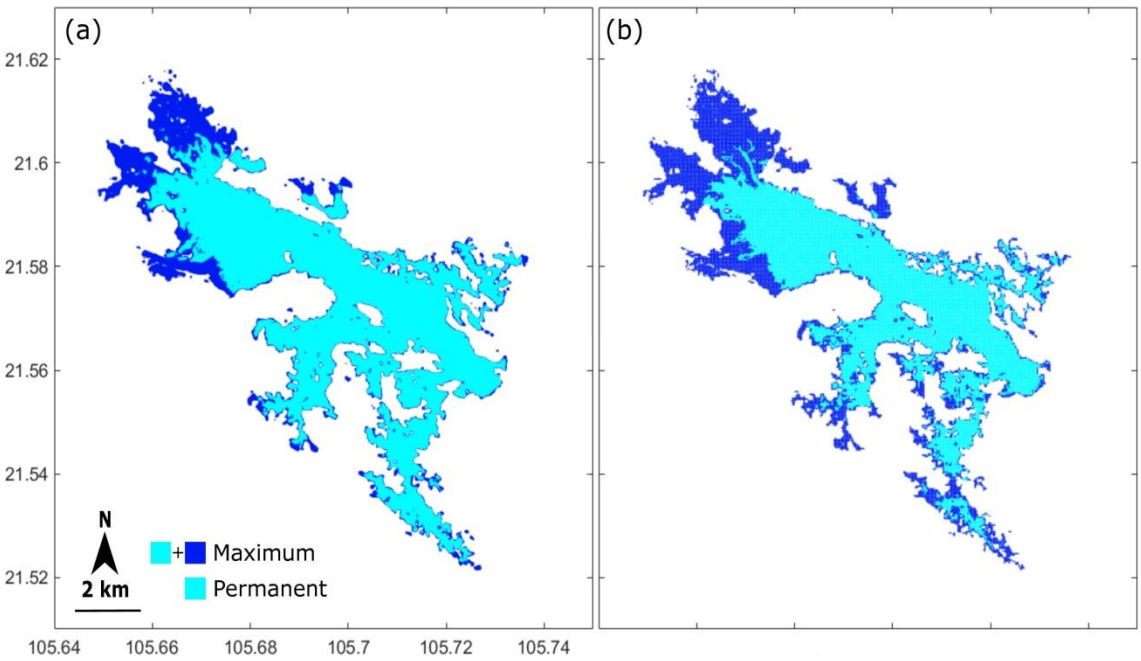


*Figure 9.* Permanent and maximum of surface water extent of Nui Coc Lake in 2019, derived from (a) Sentinel-1 observations and (b) the Global Surface Water product

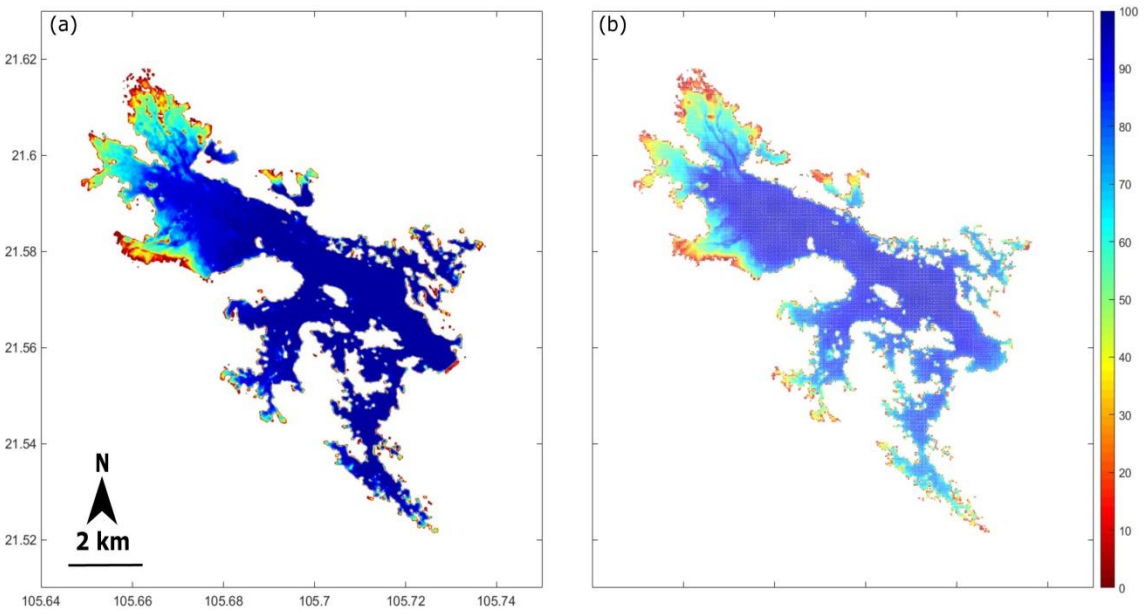


*Figure 10*. Inundation frequency of Nui Coc Lake derived from (a) Sentinel-1 observations and from (b) the Global Surface Water product

### *4.4. Comparisons with In Situ Precipitation Data*

Fig. 11 compares time series of Nui Coc Lake's surface water extent with monthly in situ data of accumulated precipitation collected at the Thai Nguyen hydro-meteorological station for the 2016-2020 period. Although Nui Coc Lake is an artificial lake, there is still a good agreement between its water extent and precipitation seasonality, with some time lag. The maximum extent of the lake is normally in September/October, occurring after the peak of rainfall in August, when water is stored inside the lake to prepare for the next crop season in the coming months. Then, the water extent reduces gradually, following the rainfall decrease during the dry season and the increase in water demand for agriculture activities. Therefore, the minimum rainfall is in February, but the minimum level of the lake is three months later in May before its extent starts to increase again when the rainy season comes.

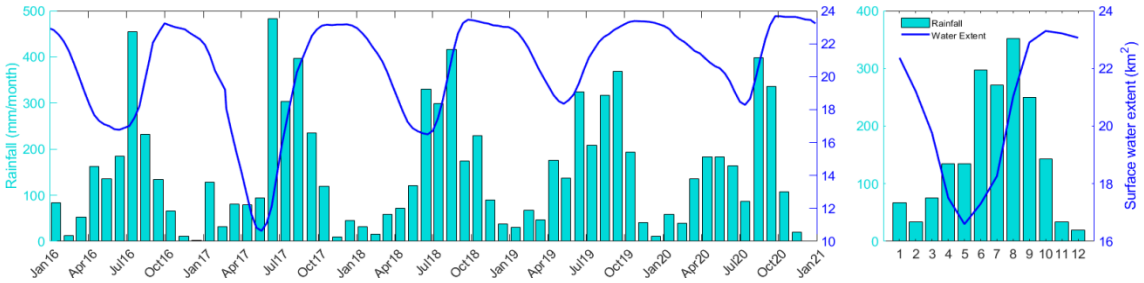


*Figure 11.* Comparison between time series of Nui Coc Lake's surface water extent derived from Sentinel-1 observations and monthly precipitation at Thai Nguyen hydro-meteorological station, for the 2016-2020 period

## 5. Discussions

The Otsu threshold algorithm is handy and effective for classifying water extent in Nui Coc Lake. We showed that the mean threshold of our image collection is -21.8 dB, with a small standard deviation (std = 0.37). However, the Otsu algorithm improves the accuracy of our method as it detects an optimal threshold for every single image. Nevertheless, it is important to note that the Otsu algorithm is only guaranteed to work well when the size of the lake and the background should be comparable, and the histogram of images should be bimodal (Fig. 3).

Agreement between surface water maps derived from SAR Sentinel-1 and free-cloud optical Sentinel-2 observations is high. The differences are mostly located at the borders between land and water, and in the northern part of the lake (see Fig. 7 and Table 3). The northern part is the most dynamic area because water from the Cong River enters the shallow part of the lake. The backscatter coefficient over shallow water might be enhanced caused by the strong wind or complex scattering mechanisms between microwave signal and the ground surface. As a consequence, our method using Sentinel-1 observations cannot classify perfectly water pixels in this part. We found that Nui Coc Lake's surface water area detected from Sentinel-1 is 4-4.5% less than that detected from Sentinel-2 (Fig. 8). Comparison with surface water maps derived from very high-resolution optical observations could help to cross-validate this finding. Unfortunately, we do not have access to these images at the moment.

The shape of the lake is similar when comparing our results with that derived from the GSW product. However, their water extent and inundation frequency maps show some differences (Fig. 9 and Fig. 10). This is as expected because the GSW product was developed based on available optical Landsat imagery. Landsat sensors might not capture the lake under cloudy conditions during rainy seasons (Mahdavi et al., 2018), while Sentinel-1 observations are not affected by weather conditions. In addition, the number of observations from 5-year Sentinel-1 observations was much more limited compared to that from 36-year Landsat observations.

This study shows the great potential of SAR Sentinel-1 observations for monitoring spatial-temporal dynamics of small lakes, especially over tropical regions where the use of optical remote sensing is normally limited (Pham-Duc et al., 2019). However, several limitations of this study can be listed. First, SAR images at HH polarization in ascending mode have the highest potential for surface water detection (Gstaiger et al., 2012). We used Sentinel-1 images in the ascending mode, but the Sentinel-1 sensor does not acquire the HH polarization. Second, VH polarization is less affected by wind that might cause the surface water roughness, compared to VV polarization. Still, a strong wind can also lead to underestimating open surface water, for instance, in the north part of the lake (Gstaiger et al., 2012). Third, aquatic, submerged, and floating vegetation might cause double-bounce and volume scatterings, which strongly influenced our classification results, especially over land/water borders (Hess et al., 1990; Pope et al., 1997). Averaging each Sentinel-1 image with the two adjacently acquired images before the final classification helps to fill out floating vegetation, as well as floating objects (boats and ships, for instance).

## 6. Conclusions and Perspective

This is the first time spatial and temporal dynamics of Nui Coc Lake, one of the largest irrigation works in North Vietnam, have been monitored using SAR Sentinel-1 observations during the 2016-2020 period. After being pre- and post-processed in the SNAP software, the

Otsu threshold algorithm was applied on each VH-polarized backscatter coefficient image to identify the optimal threshold for separating water and non-water pixels. Comparing our results with the corresponding Sentinel-2 derived surface water maps showed an overall agreement >99%, with a true positive detection of water pixels >90%. However, the surface water area detected from Sentinel-1 is 4-4.5% less than that detected from Sentinel-2 observations. The GSW product, derived from 36 years of Landsat observations, showed that radar Sentinel-1 imagery could provide consistent inundation occurrence maps compared to optical imagery. Although rainfall is one of the main sources of water entering the lake, the variation of the lake's water extent does not respond immediately to the seasonality of precipitation as there is a time lag between the two parameters. Collecting water level or discharge data of the lake will help better validate our methodology's accuracy. Unfortunately, this information was not available so far due to the lack of regular in situ measurements.

Further work could be expanded to other lakes to build a database regularly providing spatial-temporal dynamics of important lakes at a regional scale. This is important because it would help local and national governments better manage water resources in near real-time, with high spatial and temporal resolutions and low cost. The use of cloud computing platforms such as the Google Earth Engine will be investigated to save processing time. In addition, in areas where altimetry data from Sentinel-3 satellites are available, that information can be collected to estimate the lake's water volume variation, following the methodology presented in (Crétaux et al., 2011).

## Acknowledgements

This research has been supported by the basic research project from the University of Science and Technology of Hanoi, under the grant number USTH.SA.01/21 to Pham Duc Binh. The authors would like to thank the European Space Agency for providing Sentinel-1 and Sentinel-2 observations, and the Copernicus Program for providing the Global Surface Water product. We thank the Vietnam Meteorological and Hydrological Administration for providing daily in situ rainfall data of the Thai Nguyen hydro-meteorological station. We thank our colleagues, Dr. Trinh Tuan Long and Dr. Tran Anh Quan for their support in data collecting and data processing. We thank the editor and the two reviewers for their valuable comments and suggestions that helped to improve the quality of the manuscript.

## References

Acker J.G., Leptoukh G., 2007. Online analysis enhances use of NASA Earth science data. Eos, Transactions American Geophysical Union, 88(2), 14-17. https://doi.org/https://doi.org/10.1029/2007EO020003

Bartsch A., Pathe C., Wagner W., Scipa K., 2008. Detection of permanent open water surfaces in central Siberia with ENVISAT ASAR wide swath data with special emphasis on the estimation of methane fluxes from tundra wetlands. Hydrology Research, 39(2), 89-100. https://doi.org/10.2166/nh.2008.041.

Brisco B., Short N., van der Sanden J., Landry R., Raymond D., 2009. A semi-automated tool for surface water mapping with RADARSAT-1. Canadian Journal of Remote Sensing, 35(4), 336-344. https://doi.org/10.5589/m09-025.

Brisco B., Touzi R., Sanden J. J. van der, Charbonneau F., Pultz T.J., D'Iorio M., 2008. Water resource applications with {RADARSAT}-2: a preview. International Journal of Digital Earth, 1(1), 130-147. https://doi.org/10.1080/17538940701782577.

Crétaux J.-F., Abarca-del-Río, R., Bergé-Nguyen M., Arsen A., Drolon V., Clos G., Maisongrande P., 2016. Lake Volume Monitoring from Space. Surveys in Geophysics, 37(2), 269-305. https://doi.org/10.1007/s10712-016-9362-6.

Crétaux J.-F., et al., 2011. SOLS: A lake database to monitor in the Near Real Time water level and

storage variations from remote sensing data. Advances in Space Research, 47(9), 1497-1507. https://doi.org/https://doi.org/10.1016/j.asr.2011.01.004.

Dong V.T., 2017. Urgent repair of the main dam of Nui Coc Lake. Retrieved from http://dwrm.gov.vn/index.php?language=vi&nv=news&op=Tai-nguyen-nuoc/Cap-bach-sua-chua-dap-Ho-Nui-Coc-5956.

Downing J. A., et al., 2006. The global abundance and size distribution of lakes, ponds, and impoundments. Limnology and Oceanography, 51(5), 2388-2397. https://doi.org/10.4319/lo.2006.51.5.2388.

Duong T.N.T., 2012. Research on the current status and forecast the variation of water quality of Nui Coc Lake in 2020. VNU University of Science.

ESA, 2016. SAR Basics with the Sentinel-1 Toolbox in SNAP Tutorial. Retrieved from https://step.esa.int/main/doc/tutorials/sentinel-1-toolbox-tutorials/.

Filipponi F., 2019. Sentinel-1 GRD Preprocessing Workflow. Proceedings. https://doi.org/10.3390/ECRS-3-06201.s

Gstaiger V., Huth J., Gebhardt S., Wehrmann T., Kuenzer C., 2012. Multi-sensoral and automated derivation of inundated areas using TerraSAR-X and ENVISAT ASAR data. International Journal of Remote Sensing, 33(22), 7291-7304. https://doi.org/10.1080/01431161.2012.700421.

Hess L.L., Melack J.M., Simonett D.S., 1990. Radar detection of flooding beneath the forest canopy: a review. International Journal of Remote Sensing, 11(7), 1313-1325. https://doi.org/10.1080/01431169008955095.

Huth J., Gessner U., Klein I., Yesou H., Lai X., Oppelt N., Kuenzer C., 2020. Analyzing Water Dynamics Based on Sentinel-1 Time Series-a Study for Dongting Lake Wetlands in China. Remote Sensing. https://doi.org/10.3390/rs12111761.

Kuenzer C., Guo H., Huth J., Leinenkugel P., Li X., Dech S., 2013. Flood mapping and flood dynamics of the mekong delta: ENVISAT-ASAR-WSM based time series analyses. Remote Sensing, 5(2), 687-715. https://doi.org/10.3390/rs5020687.

Lehner B., Döll P., 2004. Development and validation of a global database of lakes, reservoirs and wetlands. Journal of Hydrology, 296(1-4), 1-22. https://doi.org/10.1016/j.jhydrol.2004.03.028.

Liu C., 2016. Analysis of Sentinel-1 SAR data for mapping standing water in the Twente region. Twente. Retrieved from http://www.itc.nl/library/papers%7B_%7D2016/msc/wrem/cliu.pdf.

Liu Y., Chen K.S., Xu P., Li Z.L., 2016. Modeling and Characteristics of Microwave Backscattering from Rice Canopy Over Growth Stages. IEEE Transactions on Geoscience and Remote Sensing, 54(11), 6757-6770. https://doi.org/10.1109/TGRS.2016.2590439.

Louis J., et al., 2016. SENTINEL-2 SEN2COR: L2A Processor for Users.

Mahdavi S., Salehi B., Granger J., Amani M., Brisco B., Huang W., 2018. Remote sensing for wetland classification: a comprehensive review. GIScience & Remote Sensing, 55(5), 623-658. https://doi.org/10.1080/15481603.2017.1419602.

Martinis S., Kuenzer C., Wendleder A., Huth J., Twele A., Roth A., Dech S., 2015. Comparing four operational SAR-based water and flood detection approaches. International Journal of Remote Sensing, 36(13), 3519-3543. https://doi.org/10.1080/01431161.2015.1060647.

McDonald C.P., Rover J.A., Stets E.G., Striegl R.G., 2012. The regional abundance and size distribution of lakes and reservoirs in the United States and implications for estimates of global lake extent. Limnology and Oceanography, 57(2), 597-606. https://doi.org/https://doi.org/10.4319/lo.2012.57.2.0597.

Moreira A., Prats-Iraola P., Younis M., Krieger G., Hajnsek I., Papathanassiou K.P., 2013. A tutorial on synthetic aperture radar. IEEE Geoscience and Remote Sensing Magazine, 1(1), 6-43. https://doi.org/10.1109/MGRS.2013.2248301.

Otsu N., 1979. A Threshold Selection Method from Gray-Level Histograms. IEEE Transactions on Systems, Man, and Cybernetics, 9(1), 62-66. https://doi.org/10.1109/TSMC.1979.4310076.

Ottinger M., Clauss K., Kuenzer C., 2017. Large-Scale Assessment of Coastal Aquaculture Ponds with Sentinel-1 Time Series Data. Remote Sensing. https://doi.org/10.3390/rs9050440.

Pekel J.-F., Cottam A., Gorelick N., Belward A.S., 2016. High-resolution mapping of global surface water and its long-term changes. Nature, 1-19. https://doi.org/10.1038/nature20584.

Pham-Duc B., Papa F., Prigent C., Aires F., Biancamaria S., Frappart F., 2019. Variations of Surface and Subsurface Water Storage in the Lower Mekong Basin (Vietnam and Cambodia) from Multisatellite Observations. Water, 11(1), 75. https://doi.org/10.3390/w11010075.

Pham-Duc B., Prigent C., Aires F., 2017. Surface Water Monitoring within Cambodia and the Vietnamese Mekong Delta over a Year, with Sentinel-1 SAR Observations. Water, 9(6), 366. https://doi.org/10.3390/w9060366.

Pierdicca N., Pulvirenti L., Chini M., Guerriero L., Candela L., 2013. Observing floods from space: Experience gained from COSMO-SkyMed observations. Acta Astronautica, 84, 122-133. https://doi.org/10.1016/j.actaastro.2012.10.034.

Pope K.O., Rejmankova E., Paris J.F., Woodruff R., 1997. Detecting seasonal flooding cycles in marshes of the Yucatan Peninsula with SIR-C polarimetric radar imagery. Remote Sensing of Environment, 59(2), 157-166. https://doi.org/10.1016/S0034-4257(96)00151-4.

Reschke J., Bartsch A., Schlaffer S., Schepaschenko D., 2012. Capability of C-Band SAR for Operational Wetland Monitoring at High Latitudes. Remote Sensing, 4(10), 2923. https://doi.org/10.3390/rs4102923.

Santoro M., Wegmuller U., Lamarche C., Bontemps S., Defourny P., Arino O., 2015. Strengths and weaknesses of multi-year {Envisat} {ASAR} backscatter measurements to map permanent open water bodies at global scale. Remote Sensing of Environment, 171, 185-201. https://doi.org/10.1016/j.rse.2015.10.031.

Tran M.N., 2020. Comparing low and high surface water extent of Nui Coc Lake (Vietnam) in recent years using optical remote sensing. University of Science and Technology of Hanoi.

Verpoorter C., Kutser T., Seekell D.A., Tranvik L.J., 2014. A global inventory of lakes based on high-resolution satellite imagery. Geophysical Research Letters, 41(18), 6396-6402. https://doi.org/10.1002/2014GL060641.

Voormansik K., Praks J., Antropov O., Jagomagi J., Zalite K., 2014. Flood Mapping With TerraSAR-X in Forested Regions in Estonia. IEEE Journal of Selected Topics in Applied Earth Observations and Remote Sensing, 7(2), 562-577. https://doi.org/10.1109/JSTARS.2013.2283340.

Williamson C.E., Saros J.E., Vincent W.F., Smol J.P., 2009. Lakes and Reservoirs as Sentinels, Integrators, and Regulators of Climate Change. Limnology and Oceanography, 54(6), 2273-2282. Retrieved from http://www.jstor.org/stable/20622831.

Xu H., 2006. Modification of normalised difference water index (NDWI) to enhance open water features in remotely sensed imagery. International Journal of Remote Sensing, 27(14), 3025-3033. https://doi.org/10.1080/01431160600589179.